DOI: 10.1002/chem.200600476

Chiral Poly(ureidophthalimide) Foldamers in Water

Renatus W. Sinkeldam,[a, b] Michel H. C. J. van Houtem,[a] Koen Pieterse,[a] Jef A. J. M. Vekemans,[a] and E. W. Meijer*[a]

Abstract: Poly(ureidophthalimide)s decorated with hydrophilic side chains, that ensure solubility in aqueous media, have been synthesized and characterized by UV/Vis and circular dichroism (CD) spectroscopy. Temperature and concentration dependent CD measurements in water have revealed an almost temperature and concentration independent Cotton effect, indicative for a strong intramolecular organization. Similar studies in THF demonstrate the dynamic nature of the secondary architecture, a characteristic of foldamers. In addition, the bisignated Cotton effect in water is opposite in sign to that in THF, suggestive for a solvent-dependent preference for one helical handedness. Mixing experiments prove the dominance of water in determining the handedness of the helical architecture. The solvent allows for control over the helical architecture and thus governs the supramolecular synthesis.

Keywords: chirality · foldamers · helicity · supramolecular chemistry

Introduction

The intriguing helical shape of biomolecules, with the α-helix as one of the most abundant secondary architectures in Nature, has always fascinated chemists. Native peptides are, therefore, an attractive source of inspiration to disclose the interactions reversibly inducing helicity. The numerous interactions that govern folding in natural systems have prompted chemists to design synthetic analogues to give more insight into the structural requirements for folding.[1] Closest to naturally occurring α-helices are the helical secondary structures based on β-peptides.[2] Investigations of Gellman and Seebach illustrate that modification of the β-amino acid building blocks give more control over the secondary architecture.[3,4] Even more fascinating is the finding that helical architectures comprising β-peptides are more stable than their α-peptide counterparts,[5] which is encouraging for a entirely synthetic approach. Besides the peptides or peptidomimetics also the folding of other synthetic polymers or oligomers into helical architectures are considered.[6] All of these structures belong to the class of foldamers, according to Moore, being structures reversibly folding into a conformationally ordered state in solution.[6e] Most frequently, the folding is directed by intramolecular hydrogen bonding. In several cases folding relies on solvophobicity while additional π–π stacking may stabilize the secondary architecture. Numerous strategies have been reported to arrive at non-natural foldamers. Prominent architectures are based on aromatic electron donor–acceptor couples,[7] *m*-phenylene–ethynylenes[8] and their backbone rigidified analogues,[9] aromatic oligoamides,[10–12] aromatic oligoureas,[6b,13] aromatic oligohydrazides[14] and aromatic iminodicarbonyls[15] and foldamers based on supramolecular polymers.[16] Depending on their design they may possess an inner void of sufficient size to host ions or small molecules. Obviously, mimicking nature with abiotic foldamers demands solubility in water. Natural helices constructed from α-peptides can rely on their intrinsic bipolar zwitterionic state to ensure solubility in water. However, synthetic foldamers often contain structural elements hampering solubility in an aqueous environment. The use of ionic groups in non-natural foldamers is not without consequence since it will probably also affect folding. *m*-Phenylene–ethynylenes (*m*PEs) are known for their helical secondary architectures.[8] However, it is still ambiguous whether their amphiphilic ionic counterparts adopt a helical conformation or an extended all *trans* con-

[a] Dr. R. W. Sinkeldam, M. H. C. J. van Houtem, Dr. K. Pieterse, Dr. J. A. J. M. Vekemans, Prof. Dr. E. W. Meijer
Laboratory of Macromolecular and Organic Chemistry
Eindhoven University of Technology, P. O. Box 513
5600 MB Eindhoven (The Netherlands)
Fax: (+31) 40-245-1036
E-mail: E.W.Meijer@tue.nl

[b] Dr. R. W. Sinkeldam
Current address:
Department of Chemistry and Biochemistry, University of California
San Diego, 9500 Gilman Drive, MC 0358
La Jolla, CA 92093-0358 (USA)

formation in aqueous solutions.[17,18] The best strategy is probably the use of non-ionic functionalities such as ethylene oxides to guarantee solubility in water. To our knowledge only Moore and co-workers have reported on a strategy to solubilize *m*PE foldamers in water/acetonitrile solution by decoration of the backbone with chiral[19] and achiral[20] ethylene oxide chains and in water by longer achiral[21] ethylene oxide chains. In the latter case, preference of one handedness over the other is realized by addition of a chiral guest, a small organic molecule, which fits in the inner void of the foldamer. This beautiful example demonstrates the potential of synthetic foldamers as candidates for mimicking biological functions. Besides the use of *m*PEs as a host, similar experiments albeit not in water, with aromatic oligoamides have been reported.[22] With the use of oligo(ureido–*meta*-phenylene)s even mimicking of transmembrane ion channels is anticipated.[6b,23] In that case the urea functions adopt a cisoid conformation due to intramolecular hydrogen bonding between the urea hydrogens and the carbonyl of an adjacent ester functionality.

Previously we have reported on a poly(ureido-*para*–phthalimidyl) foldamer in which the urea N-H groups adopt a cisoid conformation.[24] In that case the consecutive monomeric units introduce a curvature in the ureidophthalimide backbone due to intramolecular hydrogen bonding of urea protons with the adjacent imide carbonyls. This interaction induces a bend of somewhat larger than 120°, and thus nucleates folding (Figure 1). Due to the *para* substitution in the phthalimide unit a larger inner void is created upon folding than in the oligo(ureido–*meta*-phenylene) system.

CD studies of the polymer in THF indicate folding into a helical architecture. Moreover, studies in heptane indicate the stacking of shorter oligomers to larger chiral aggregates. However, the same compound dissolved in $CHCl_3$ proves to be CD silent and is regarded as residing in the non-folded state.

Similar to the work of Moore, the oligo(ureidophthalimide) foldamer presented in this paper also relies on oligo(ethylene oxide) functionalities to ensure solubility in water. Recently, we reported a general synthetic strategy towards

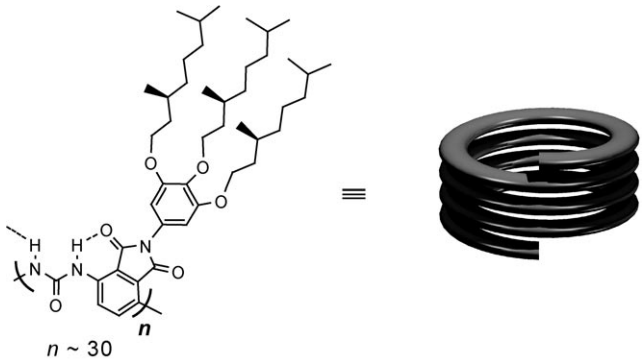

Figure 1. Folding in poly(ureidophthalimide) induced by intramolecular hydrogen bonding.

an array of 3,6-diaminophthalimides,[25] the building blocks for the foldamers. In this way chiral oligo(ethylene oxide) side chains have been incorporated in the foldameric structure enabling a CD study—after isolation of the high molecular weight fraction—of the polymer in aqueous solution.

Results and Discussion

The ureidophthalimide based polymer **3** was obtained by reaction of diamine **1** with diisocyanate **2** in refluxing dioxane in the presence of one equivalent of 4-dimethylaminopyridine (DMAP) (Scheme 1).

Previously, an efficient synthetic approach to tosylated (2*S*)-2-methyl-3,6,9,12,15-pentaoxahexadecanol (**4**) and its coupling to methyl gallate **5** have been described (Scheme 2).[26] Subsequently, methyl ester **6** was hydrolyzed and the acid converted to the acid chloride,[26] which was treated with sodium azide to acyl azide **7**. Curtius rearrangement in dioxane at elevated temperatures rendered isocyanate **8**, which in turn was hydrolysed to the corresponding amine **9** by slow addition to aqueous potassium hydroxide in dioxane at 90 °C.

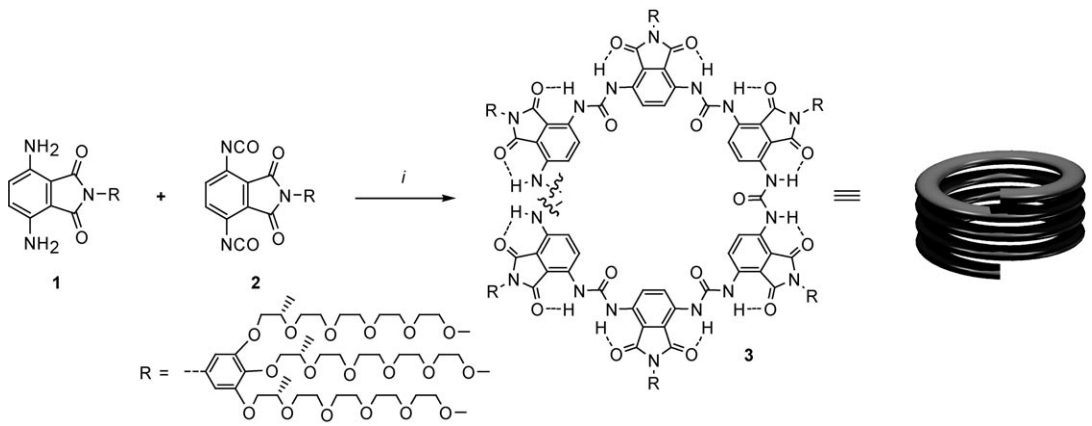

Scheme 1. Polymerization of diamine **1** with diisocyanate **2**. i) DMAP (1 equiv), dioxane, reflux, 17 h.

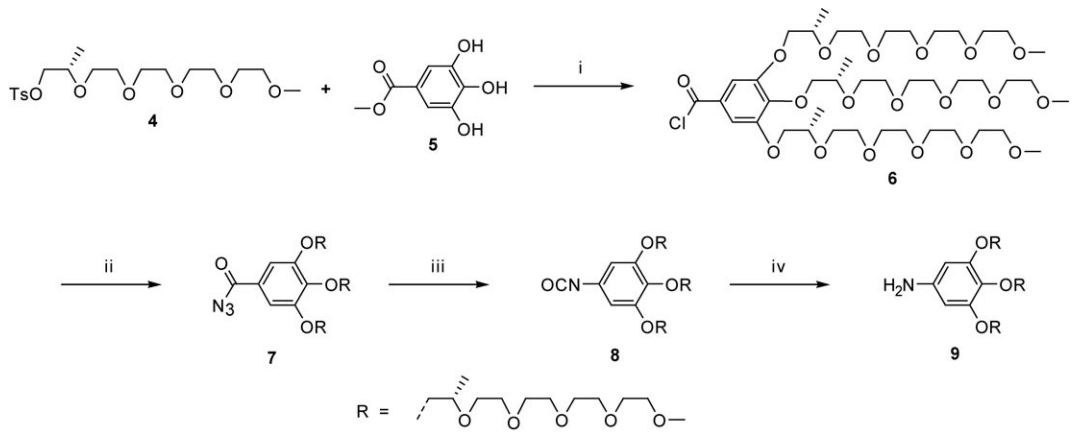

Scheme 2. Synthesis of amine **9**. i) **4** (3.05 equiv), **5**, K_2CO_3 (6.2 equiv), Bu_4NBr (0.05 equiv), MIBK, reflux, 6 h; KOH (3.3 equiv), EtOH/H_2O 1:1, reflux, 17 h; 0.1 M HCl until pH ~3, 95%; $(COCl)_2$ (1.2 equiv), DMF (5 drops), CH_2Cl_2, RT, 17 h, 99%;[26] ii) NaN_3 (18 equiv), THF/H_2O 1:1, 5°C, 1 h, 99%; iii) dioxane, reflux, 4 h, ~100%; iv) KOH (160 equiv), H_2O, 90°C, 30 min, 97%. MIBK = methylisobutylketone.

The chirality in oligo(ethylene oxide) **4** was introduced by starting from ethyl (*S*)-(−)-lactate (purity of 98%) of which the *ee* value was determined by gas chromatography (GC) on a capillary column with a permethylated β-cyclodextrin stationary phase yielding an *ee* > 99.5%.[27] Part of the routes is based on earlier work that also showed the fidelity of keeping the enantiomeric excess as high as the starting materials.[28]

Amine **9** was converted into the phthalimide synthon **11** by reaction with 3,6-bis(acetylamino)phthalic anhydride **10** (Scheme 3).[29,25] Removal of the acetyl functions to afford the corresponding diamine **1** was achieved by exposure of diamide **11** to 1.5 M aqueous HCl in refluxing dioxane followed by neutralization. Subsequent treatment of diamine **1** with 20 wt% phosgene in toluene afforded diisocyanate **2**. The conversion was monitored by IR spectroscopy and proved to be complete and quantitative after 30 minutes at room temperature.

Polymerization of diamine **1** with diisocyanate **2** according to Scheme 1 furnished ureidophthalimide polymer **3**. Monitoring the polymerization by IR spectroscopy indicated that the reaction was finished after 17 h in refluxing dioxane when all diisocyanate was consumed. The non-migrating DMAP was removed by filtration over silica gel upon elution with a solvent mixture of 10% methanol in 1,2-dimethoxyethane. A separation of shorter and longer oligomers was effectuated by column chromatography over silica gel with a solvent mixture gradient from 1 to 10% methanol in 1,2-dimethoxyethane. Due to the polar nature of the oligo(ethylene oxide) tails, the first fraction (**3a**) was a mixture of predominantly short oligomers with a small amount of longer oligomers. The second fraction (**3b**) contained only oligomers longer than eight units. The difference in polymeric distribution has been established on GPC ($CHCl_3$, mixed-E column, detection at 310 nm). Fraction **3a** had a longer elution time (max. 5.69 min) than fraction **3b** (max. 4.37 min). Furthermore, from ^1H NMR endgroup analysis

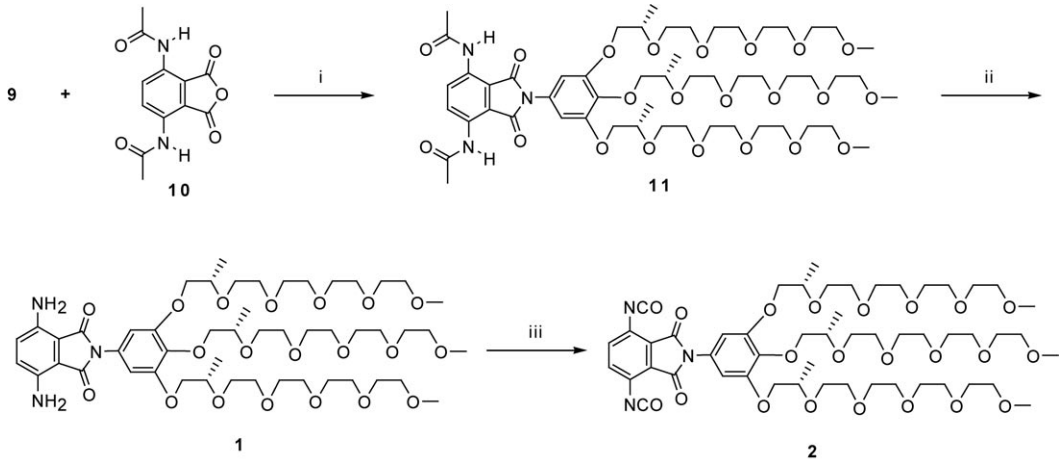

Scheme 3. Syntheses of polymer building blocks **1** and **2**. i) Dioxane, reflux, 17 h, 90%; ii) dioxane/water/HCl (12 M) 6:1.5:1, 90°C, 45 min, 95%; iii) $COCl_2$ (40 equiv), $PhCH_3$, RT, 2.5 h, ~100%.

on the latter an average degree of polymerization has been deduced of 20 units, that is, an M_n of 21450 g mol^{-1} has been estimated.

Previous studies on ureidophthalimide based polymers have been restricted to organic solvents such as heptane, chloroform and THF due to the apolar periphery. For such systems the largest Cotton effect was observed in THF.[24] However, the polar nature of the oligo(ethylene oxide) tails present in **3b** ensured solubility in water. Thus, a dilute aqueous solution of the high molecular weight fraction **3b** was subjected to a UV/Vis and CD study. The transparency of water allowed to investigate a spectral ranging from 190 to 500 nm. The UV/Vis spectrum shows three distinct absorption maxima located at 209 (with a shoulder at 230 nm), at 312 and 398 nm (Figure 2).

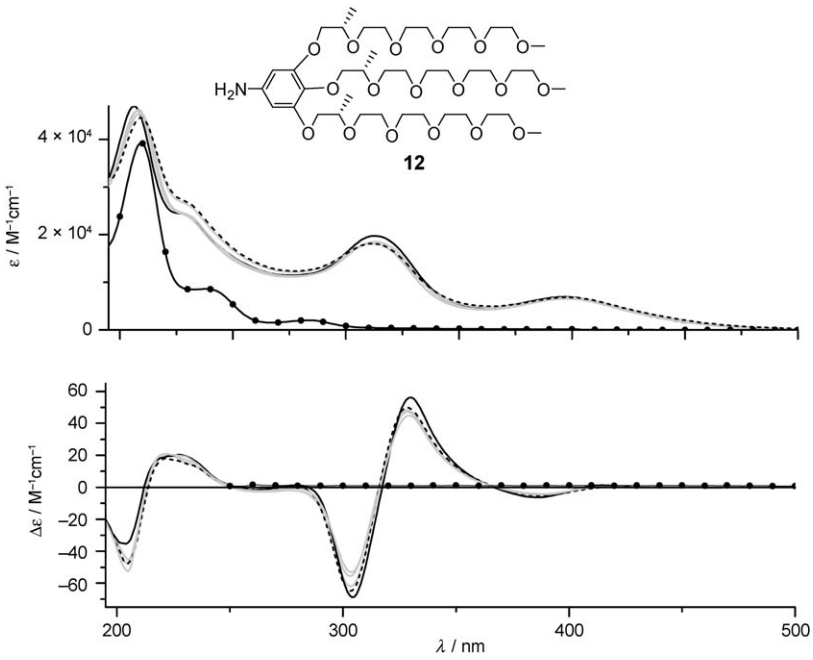

Figure 2. Temperature dependent UV/Vis and CD spectra of **3b** in water (4.7×10^{-5} M), 15 °C (black line), 90 °C (dashed line), and intermediate temperatures (grey lines), and absorption spectrum of amine **12** (closed circles).

The absorptions located at 310 and 398 nm can be attributed to the phthalimide part of the structure by comparison with the absorption spectrum of amine **12**. In CD spectroscopy two bisignate Cotton effects were observed. The first bisignate effect displayed maxima of $\Delta\varepsilon = -53\,M^{-1}cm^{-1}$ ($g_{abs} = -0.0012$) at 205 nm and $\Delta\varepsilon = +21\,M^{-1}cm^{-1}$ ($g_{abs} = 0.0009$) at 222 nm (Figure 2). The zero-crossing at 213 nm coincides with the absorption maximum in the UV/Vis spectrum. The second bisignate Cotton effect displays maxima with $\Delta\varepsilon = -69\,M^{-1}cm^{-1}$ ($g_{abs} = -0.0040$) at 304 nm and $\Delta\varepsilon = +56\,M^{-1}cm^{-1}$ ($g_{abs} = 0.0045$) at 330 nm. The zero-crossing at 318 nm coincides with the absorption maximum of the phthalimide unit in UV/Vis spectrometry. Additionally a small negative CD effect was observed that relates to the absorption at 398 nm and is presumably to be attributed to the terminal amino end capped phthalimide. It must be noted that 3,6-diaminophthalimide **1** as well as its precursor 3,6-bis(acetylamino)phthalimide **11** proved to be CD silent in water.

The appearance of a Cotton effect in water is remarkable since the folding is designed to be directed by intramolecular hydrogen bonding of the urea protons with the imide carbonyl oxygens. Preliminary molecular modelling studies in vacuo of a section of a poly(ureidophthalimide) helix ($n = 30$) showed a cone-like structure (Figure 3). It indicates that seven units per turn create an inner part of approximately 14 Å. The cisoid conformation is apparent, while π–π stacking was observed reminiscent to that of helicenes. It is safe to state that initial folding is driven by shielding the apolar core from the polar solvent. This solvophobic effect

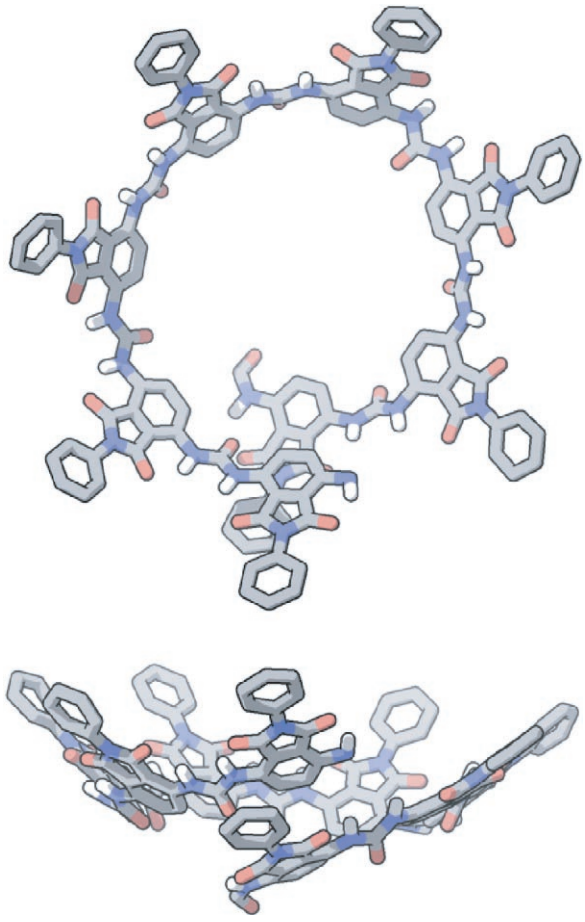

Figure 3. Top and side view of a section of a poly(ureidophthalimide) helix after a 1 ns molecular dynamics simulation in vacuo at 300 K. Tails and C-H protons are omitted for clarity.

creates a hydrophobic microdomain which allows the expression of subtle hydrogen-bonding interactions. Once initiated the system is templated towards folding since the favorable hydrophobic pocket, secured by π–π stacking, is already there. In addition, although variations were observed, the intensity of the Cotton effect was hardly affected by raising the temperature. The remarkable stability of this folded structure in water contrasts to many native helix-forming proteins which are only marginally stable in water.[30,31] The extreme stability in water is easily explained by the strong hydrophobic forces and π–π interaction hampering the structure to be water-soluble in its unfolded form. The significant CD effects are attributed to supramolecular chirality and strongly support the presence of a helical architecture.

The oligo(ethylene oxide)-rich periphery of **3b** does not restrict the solubility of **3b** to water alone. Thus, a dilute solution of **3b** in freshly distilled THF has been subjected to a UV/Vis and CD spectroscopy study. The width of the spectral window was reduced to approximately 250 nm. The UV/Vis spectrum revealed two absorption maxima located at 315 and 394 nm (Figure 4).

The CD spectrum of the same solution shows a Cotton effect with a $\Delta\varepsilon$ of $+24\,\mathrm{M^{-1}cm^{-1}}$ ($g_{abs}=0.0009$) at 313 nm and $\Delta\varepsilon=-17\,\mathrm{M^{-1}cm^{-1}}$ ($g_{abs}=0.0017$) at 331 nm, respectively, with a zero-crossing at 323 nm. In contrast to the temperature dependent CD measurements in water, the Cotton effect in THF decreased upon raising the temperature and completely vanished at 55 °C. The original value was reclaimed upon cooling to room temperature illustrating the dynamics of the system in THF. The loss of the Cotton effect at elevated temperatures may be attributed to the unfolding of the helical architecture into a random coil conformation or mark the attained equilibrium between *P* and *M* helices. The latter seems to be in agreement with the spectral behavior at different temperatures. Elevation of the temperature does not result in a shift of the absorption maximum, which implies that there is no evidence for a change in the aromatic packing.[32] Moreover, the presence of an isodichroic point throughout the temperature dependent measurements in THF indicates that the structure does not adopt other conformations or aggregation states.[19a] A melting curve (Figure 4, right) could be constructed from the temperature dependent CD data. An exponential function represented by a grey line adequately fits the data points. The slope of the curve, denoted by the black line, enables estimation of the change in enthalpy involved in this process. Applying the formula $\Delta H = \mathrm{slope}\cdot T^2$ gives $\Delta H = -5.5\,\mathrm{kJ\,mol^{-1}}$.

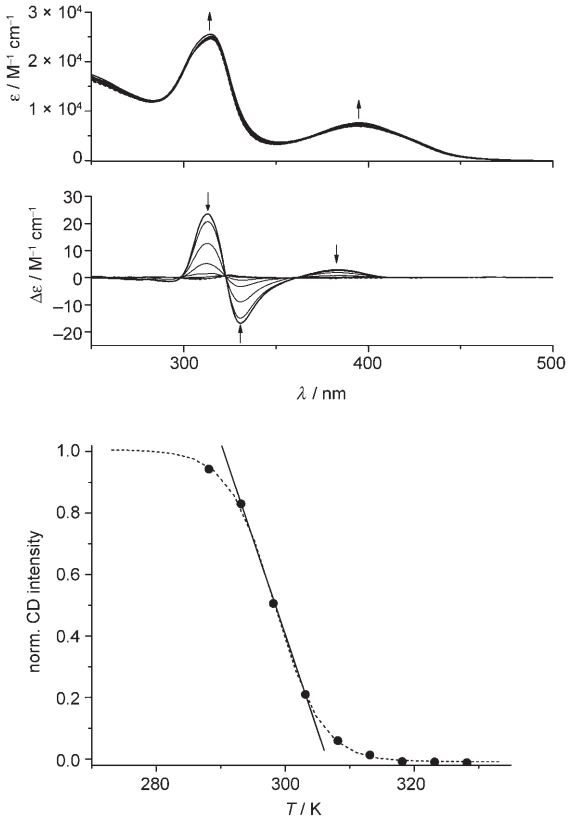

Figure 4. Top: Temperature dependent CD (upper) and UV/Vis (lower) spectra of **3b** in THF (5.0×10^{-5} M) from 15 °C (black line) to 55 °C (dashed line) with steps of 5 °C (grey lines). Bottom: melting curve constructed from the CD intensity at 320 nm (black circles), a fitted exponential curve (dashed line) and a straight line representing the slope (black line).

The comparison of **3b** in THF and in water shows that the Cotton effect in THF is smaller and of opposite sign compared to the measurement in water. The lower intensity of the CD effect in THF can point to a less tight packing of the chromophores and/or less intermolecular aggregation of the helical architectures. The latter possibility is addressed with concentration dependent CD studies in water and THF, which does not reveal a strong correlation between concentration and CD intensity over a 100 fold concentration range (10^{-4} to 10^{-6} M), implying that in THF and in water only monomolecular species are present (Figure 5).

This is supported by temperature dependent gel permeation chromatography experiments in THF (Figure 6). Measurements at 55 °C show even a shift to shorter retention times compared with measurements at 25 °C, strongly suggesting the absence of aggregation.

Hence, the less intense Cotton effect in THF can most likely be attributed to looser packing of the aromatic system. This is supported by a 23 % higher molar extinction coefficient of **3b** at 314 nm in THF compared with the overall optical density in water. Hypochromicity is a convincing indication of a tighter packing of the chromophores and is also observed in DNA, RNA and other polymers.[33] The observed hypochromic effect can be rationalized by the properties of the solvent. THF is a good solvent for both the apolar core and the polar oligo(ethylene oxide) periphery. However, water can only dissolve the polar oligo(ethylene oxide) periphery and will force the apolar core to minimize exposure to water by tight folding and as a consequence induces tight packing of the aromatic units.

The opposite sign of the Cotton effect in THF compared with water hints towards inversion of the helical handedness.

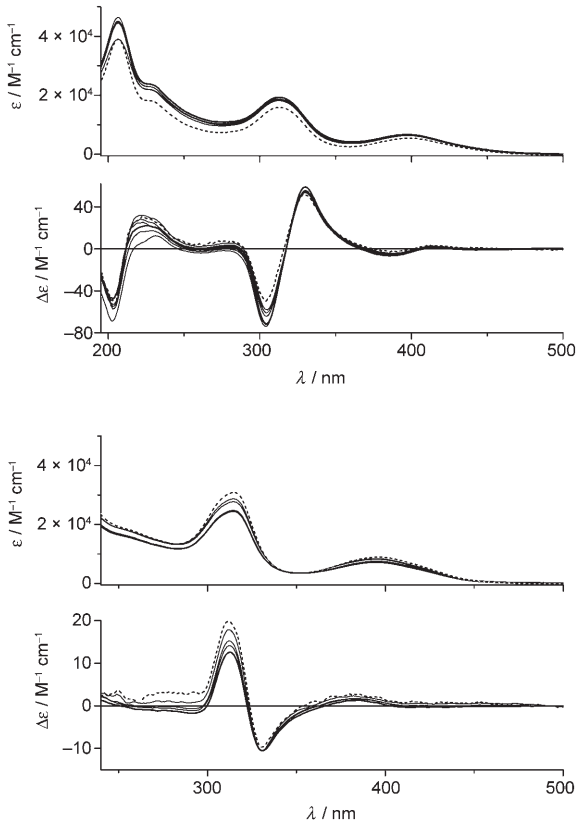

Figure 5. Concentration dependent CD measurements of **3b** at 20 °C from 5.0×10^{-4} M (thick black line) to 5.0×10^{-6} M (dashed line) in 5 steps (black lines) in water (top) and in THF (bottom).

Solvent induced inversion of helicity in macromolecular systems has been reported previously.[34] In this case the effect might be attributed to differences in hydrogen-bonding interactions with the two solvents and a different conformation of the chiral oligo(ethylene oxide) side chains. There is a preference for a *gauche* conformation along the C–C axis and for a *trans* conformation along the C–O axis of the oligo(ethylene oxide) tails in water, as has been established by Matsuura et al. with detailed IR spectroscopy studies on poly(ethylene oxide).[35] Recently a similar effect was reported in dendrons decorated with chiral oligo(ethylene oxide) tails that show an opposite Cotton effect in water compared with THF.[36] Therein, this effect is explained as a helical *M* → *P* transition upon going from THF to water. To investigate the relative influence of the solvent on the helical architecture, **3b** is studied in THF/water mixtures, keeping the concentration constant. From the UV/Vis spectra it becomes clear that the optical density in pure water is increased upon addition of the THF solution (Figure 7). This suggests loosening of the intramolecular packing, which eventually might permit helix inversion.

The accompanying CD spectra show that upon increasing the THF/water ratio the Cotton effect gradually decreases. It is quite remarkable that over 99 vol% of THF in water is required to reach inversion of the Cotton effect. These findings demonstrate the dominant influence of water on the

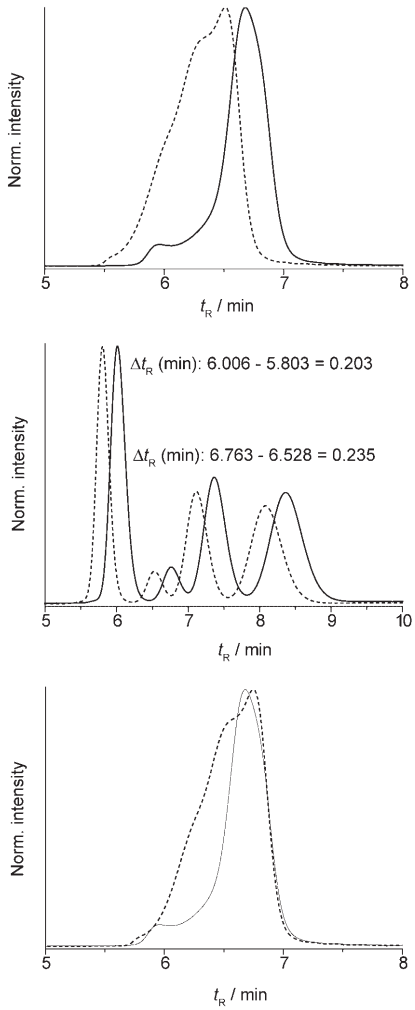

Figure 6. GPC chromatograms at 25 °C (solid line) and 55 °C (dashed line) of **3b** uncorrected (top); PSMP (polystyrene) standard, M_w: 30300, 10150, 5000 and 1600 (middle); **3b** with correction of PSMP M_w 10150 (uncorrected curve of **3b** + 0.235 minutes; bottom).

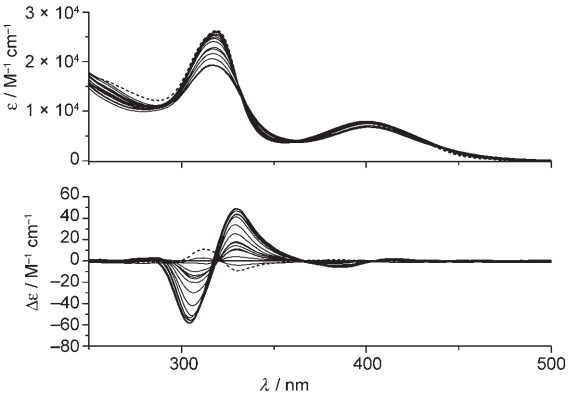

Figure 7. CD (top) and UV/Vis (bottom) spectra of mixing of **3b** in THF (dashed line) with a solution of **3b** in water (thick black line) in 10% steps (intermediate lines) keeping the concentration constant at 4.2×10^{-5} M. Every curve represents a new mixture of **3b** in THF with **3b** in water and hence does not equal a titration.

conformation of the secondary architecture. This is in line with the insensitivity of the Cotton effect in water to temperature changes (Figure 2).

Conclusion

A novel hydrophilic ureidophthalimide polymer has been synthesized that establishes a folding dynamics in THF and that reveals outstanding stability of the putative helical architectures in water. Circular dichroism studies at different concentrations show a concentration independent Cotton effect, indicative for intramolecular folding. Temperature dependent GPC measurements in THF suggest the absence of intermolecular aggregation. The opposite Cotton effect observed in water compared with THF indicates a solvent induced preference for helical handedness. Titration experiments with water/THF mixtures denote the dominant influence of water on the handedness. Furthermore, the assumed helical inversion allows control over the diastereomeric excess. The dimensions of the hollow core created by folding, may allow the hosting of ions and may even be suitable for accommodation of small molecules. Our future research will focus on the potential exploitation of the inner void.

Experimental Section

General experimental: All solvents used were provided by Biosolve and of AR quality. Dry tetrahydrofuran was obtained by distillation from Merck 4 Å molecular sieves. 1,2-Dimethoxyethane was purchased from Acros and purified by distillation. 4-Dimethylaminopyridine was obtained from Aldrich and was used as stock solution in distilled dioxane containing molecular sieves (4) Å). Phosgene was purchased from Fluka as a 20 wt% solution in toluene. ^{1}H and ^{13}C NMR spectra were recorded on a Varian Mercury, 400 MHz for ^{1}H NMR and 100 MHz for ^{13}C NMR, or on a Varian Gemini, 300 MHz for ^{1}H NMR and 75 MHz for ^{13}C NMR. Proton chemical shifts are reported in ppm downfield from tetramethylsilane (TMS) and carbon chemical shifts in ppm downfield from TMS using the resonance of the deuterated solvent as internal standard. IR spectra were obtained using a Perkin–Elmer Spectrum One ATR-FTIR machine. UV/vis spectra were measured on a Perkin–Elmer Lambda 40 spectrometer, using (HELMA) quartz cuvettes (path length 1 cm). Circular dichroism spectra were recorded on a Jasco J600 equipped with a Jasco PTC-348WI temperature controller. All ε and $\Delta\varepsilon$ values were calculated per mole monomeric phthalimide units. Matrix assisted laser desorption/ionization mass spectra were obtained using α-cyano-4-hydroxycinnamic acid as the matrix on a PerSeptive Biosystems Voyager-DE PRO spectrometer. Elemental analyses were carried out using a Perkin–Elmer 2400. All moisture sensitive reactions were performed under an atmosphere of dry argon. Analytical thin layer chromatography was performed on Kieselgel F-254 precoated silica gel plates. Visualization was accomplished with UV light. Column chromatography was carried out on Merck silica gel 60 (70–230 mesh or 230–400 mesh ASTM). GPC measurements on the oligomeric mixtures were performed on a mixed D column (PL gel 5 μm, 200–400 000 g mol^{-1}), with a flow of 1 mL min^{-1}, and chloroform as the eluting solvent. The injection volume was 50 μL and UV detection (254 or 310 nm) was applied. Molecular weights and polydispersity indices were calculated from a polystyrene standard.

3,4,5-Tris[(2*S*)-2-(2-{2-[2-(2-methoxyethoxy)ethoxy]ethoxy}ethoxy)propoxy]benzoyl azide (7): Under argon, gallic acid chloride **6**[26] (7.88 g, 8.441 mmol) was dissolved in THF (23 mL) and slowly added to an ice-cold suspension of NaN_3 (10.09 g, 0.155 mol) in water (23 mL) keeping the temperature below 5 °C. After addition, the mixture was stirred for 1 h and THF was evaporated in vacuo at RT. The aqueous residue was extracted with dichloromethane (4×100 mL), the combined organic layers were dried over $MgSO_4$ and filtered followed by concentration of the filtrate in vacuo, yielding **7** (4.354 g, 4.621 mmol, 99%) as a light brown thick oil that was used as such. ^{1}H NMR (400 MHz, $CDCl_3$, 25 °C): δ = 7.31 (s, 2H, a), 4.14–4.04 (3H, b), 3.96–3.85 (5H, c), 3.81–3.69 (7H, d), 3.68–3.58 (36H, e), 3.56–3.53 (6H, f), 3.37 (s, 9H, g), 1.31–1.27 ppm (9H, h); FT-IR (ATR): $\tilde{\nu}$ = 2870, 2143, 1686, 1584/1498, 1453/1429, 1331, 1298, 1236, 1194, 1098, 1036, 935, 853, 808, 743, 666 cm^{-1}.

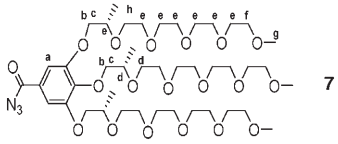

5-Isocyanato-1,2,3-tris[(2*S*)-2-(2-{2-[2-(2-methoxyethoxy)ethoxy]ethoxy}ethoxy)propoxy]benzene (8): Under argon, gallic acyl azide **7** (2.368 g, 2.513 mmol) was dissolved in dioxane (50 mL) and heated under reflux for 4 h. Analysis by IR spectroscopy proved full conversion to the isocyanate **8**. The solution was used as such in the next step. FT-IR (ATR): $\tilde{\nu}$ = 2870, 2263, 1591/1514, 1452/1425, 1374, 1350, 1301, 1228, 1200, 1099, 1022, 942, 848, 677 cm^{-1}.

3,4,5-Tris[(2*S*)-2-(2-{2-[2-(2-methoxyethoxy)ethoxy]ethoxy}ethoxy)propoxy]aniline (9): Under argon, isocyanate **8** (2.292 g, 2.513 mmol) in dioxane (50 mL) was slowly added through a cannula to a hot (60 °C), well-stirred solution of KOH (22.44 g, 0.40 mol, an excess is used to minimize urea formation) in water (200 mL), which was purged with nitrogen gas for 0.5 h prior to use. After addition of the isocyanate the mixture was stirred at 90 °C under argon for 0.5 h and then concentrated in vacuo to remove the dioxane. The aqueous residue was extracted with CH_2Cl_2 (3× 75 mL). The combined organic layers were dried over $MgSO_4$, filtered and concentrated in vacuo. Under argon the residue was mixed with a solution of NaOH (8.0 g, 0.20 mol) in water (100 mL) and dioxane (40 mL), which was purged with nitrogen for 30 minutes before use. The stirred reaction mixture was heated under reflux for 3 d to hydrolyze the small amount of urea present in the mixture. Then, the mixture was allowed to reach room temperature and brine (10 mL) was added. Subsequently, the mixture was extracted with CH_2Cl_2 (3×75 mL), the combined organic layers dried over $MgSO_4$ and the suspension filtered. Concentration of the filtrate in vacuo gave **9** (2.169 g, 2.447 mmol, 97%) as a thick brownish oil that was used as such. R_f = 0.41 (silica gel, 1,2-dimethoxyethane); HPLC (PDA detector): t_R = 2.33 min, purity ~97%. ^{1}H NMR (400 MHz, $CDCl_3$, 25 °C): δ = 5.93 (s, 2H, a), 3.99 (m, 2H, b), 3.92 (m, 1H, c), 3.85–3.69 (12H, d), 3.67–3.61 (36H, e), 3.58–3.53 (6H, f), 3.38 (s, 9H, g), 1.28–1.26 ppm (9H, h); ^{13}C NMR (50 MHz, $CDCl_3$, 25 °C): δ = 153.4 (C1), 143.2 (C2), 130.7 (C3), 94.8 (C4), 76.8 (C5), 75.2 (C6), 74.6 (C7), 72.8 (C8), 72.1 (C9), 71.1–70.7 (C10), 69.0 (C11), 68.7 (C12), 59.3 (C13), 18.0–17.8 ppm (C14); FT-IR (ATR): $\tilde{\nu}$ = 3362, 2870, 2160, 1608, 1507, 1453, 1374, 1350, 1294, 1237, 1200, 1096, 1025, 945, 849, 737 cm$^{-1;}$ MALDI-TOF MS: *m*/*z* (%): calcd for: 885.53; found: 885.73 (100) $[M]^+$, 908.72 (55) $[M+Na]^+$, 924.74 (10) $[M+K]^+$; Elemental analysis calcd (%) for $C_{42}H_{79}NO_{18}$: C 56.93, H 8.99, N 1.58; found: C 56.61, H 9.00, N 1.53.

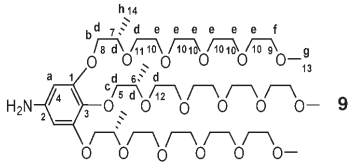

3,6-Bis(acetylamino)-*N*-{3,4,5-tris[(2*S*)-2-(2-{2-[2-(2-methoxyethoxy)-ethoxy]ethoxy}ethoxy)propoxy]phenyl}phthalimide (11): Under argon,

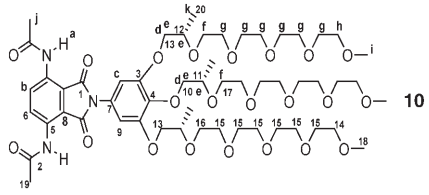

10

3,6-bis(acetylamino)phthalic anhydride **10**[25] (0.377 g, 1.438 mmol) and amine **9** (1.333 g, 1.504 mmol) were mixed in dioxane (7.2 mL). After 17 h reflux the mixture was concentrated in vacuo and the remaining residue was purified by column chromatography (silica gel, 25 vol% heptane in 1,2-dimethoxyethane) yielding **11** (1.457 g, 1.289 mmol, 90%) as a yellow thick oil. $R_f = 0.31$ (silica gel, 20 vol% heptane in 1,2-dimethoxyethane). $t_R = 8.38$ min (GPC, mixed D, 254 nm, $CHCl_3$). ^{1}H NMR (400 MHz, $CDCl_3$, 25 °C): $\delta = 9.38$ (s, 2H, a), 8.81 (s, 2H, b), 6.62 (s, 2H, c), 4.10–4.02 (3H, d), 3.90–3.81 (6H, e), 3.77–3.69 (6H, f), 3.68–3.62 (36H, g), 3.56–3.52 (6H, h), 3.39–3.37 (s, 9H, i), 2.26 (s, 6H, j), 1.32–1.29 ppm (9H, k); ^{13}C NMR (50 MHz, $CDCl_3$, 25 °C): $\delta = 169.0$ (C1), 168.3 (C2), 152.9 (C3), 138.0 (C4), 133.3 (C5), 127.5 (C6), 126.0 (C7), 113.8 (C8), 105.6 (C9), 76.4 (C10), 75.1 (C11), 74.4 (C12), 72.8 (C13), 72.0 (C14), 70.9–70.5 (C15), 68.9 (C16), 68.6 (C17), 59.1 (C18), 24.9 (C19), 17.7–17.5 ppm (C20); FT-IR (ATR): $\tilde{\nu}$ = 3363, 2871, 2184, 1754, 1699, 1637, 1616, 1548, 1598, 1491, 1438, 1393, 1369, 1297, 1239, 1200, 1099, 1016, 978, 906, 845, 762, 688, 665 cm^{-1}; UV/Vis (H_2O, 4.87×10^{-5} mol L^{-1}): λ_{max} (ε) = 259 (24000), 367 nm (4500 mol^{-1} dm^{-3} cm^{-1}); MALDI-TOF MS: *m*/*z* (%): calcd for: 1152.57, found: 1152.65 (100) $[M+Na]^+$, 1169.61 (22) $[M+K]^+$; elemental analysis calcd (%) for $C_{54}H_{87}N_3O_{22}$: C 57.38, H 7.76, N 3.72; found: C 57.41, H 7.78, N 3.61.

3,6-Diamino-*N*-{3,4,5-tris[(2*S*)-2-(2-{2-[2-(2-methoxyethoxy)ethoxy]-ethoxy}ethoxy)propoxy]phenyl}phthalimide (1): Under argon, 3,6-bis-(acetylamino)phthalimide **11** (1.247 g, 1.104 mmol) was dissolved in a

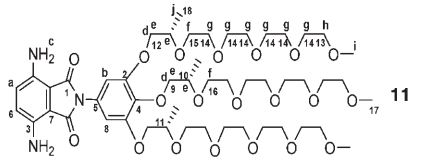

11

mixture of dioxane, water and HCl (12 M) (4.2 mL/1.1 mL/0.7 mL). The stirred reaction mixture was heated at 90 °C for 45 min, and then poured into ice-water. Subsequently, satd aq $NaHCO_3$ solution and brine were added, adjusting the pH to 8. The aqueous mixture was then extracted with CH_2Cl_2 (4 × 75 mL), the combined organic layers were dried over $MgSO_4$ and the filtrate concentrated in vacuo. The residue was purified by column chromatography (silica gel, 10 vol% heptane in 1,2-dimethoxyethane, $R_f = 0.3$) yielding **1** (1.150 g, 1.099 mmol, 95%) as an orange thick oil. $t_R = 8.58$ min (GPC, mixed D, 254 nm, $CHCl_3$); $t_R = 8.93$ min (HPLC, PDA), purity > 97%; ^{1}H NMR (400 MHz, $CDCl_3$, 25 °C): $\delta = 6.81$ (s, 2H, a), 6.65 (s, 2H, b), 5.00 (s, 4H, c), 4.08–4.02 (3H, d), 3.90–3.78 (6H, e), 3.78–3.68 (6H, f), 3.68–3.59 (36H, g), 3.56–3.53 (6H, h), 3.38–3.36 (s, 9H, i), 1.31–1.27 ppm (d, 9H, j); ^{13}C NMR (50 MHz, $CDCl_3$, 25 °C): $\delta = 168.4$ (C1), 152.5 (C2), 138.8 (C3), 137.1 (C4), 127.5 (C5), 125.5 (C6), 108.3 (C7), 105.8 (C8), 76.3 (C9), 75.0 (C10), 74.3 (C11), 72.6 (C12), 71.9 (C13), 70.8–70.4 (C14), 68.8 (C15), 68.5 (C16), 59.0 (C17), 17.7–17.5 ppm (C18); FT-IR (ATR): $\tilde{\nu}$ = 3465, 3355, 2871, 2179, 1732, 1688, 1656, 1619, 1595, 1494, 1434, 1374, 1350, 1292, 1242, 1190, 1094, 1025, 941, 829, 767, 730, 706 cm^{-1}; UV/Vis (H_2O, 4.21×10^{-5} mol L^{-1}): λ_{max} (ε) = 260 (13100), 448 nm (7400 mol^{-1} dm^{-3} cm^{-1}); MALDI-TOF MS: *m*/*z* (%): calcd for: 1045.56, found 1045.47 (8) $[M]^+$, 1068.47 (100) $[M+Na]^+$, 1084.45 (13) $[M+K]^+$; elemental analysis calcd (%) for $C_{50}H_{83}N_3O_{20}$: C 57.40, H 8.00, N 4.02; found: C 57.48, H 8.14, N 4.02.

3,6-Diisocyanato-*N*-{3,4,5-tris[(2*S*)-2-(2-{2-[2-(2-methoxyethoxy)ethoxy]-ethoxy}ethoxy)propoxy]phenyl}phthalimide (2): Under argon, 3,6-diaminophthalimide **1** (0.157 g, 0.150 mmol) was dissolved in dry toluene (2.0 mL). A phosgene solution (3.75 mL, 7.09 mmol of a 20 w% solution

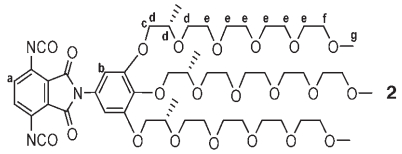

2

in $PhCH_3$) was slowly added to the reaction mixture under continuous stirring. After addition the reaction mixture was stirred for 2.5 h at room temperature. Subsequent concentration in vacuo gave **2** (0.165 g, ~100%) as a thick dark-yellow oil that was used as such. ^{1}H NMR (400 MHz, $CDCl_3$, 25 °C): $\delta = 7.29$ (s, 2H, a), 6.62 (s, 2H, b), 4.08–4.02 (3H, c), 3.89–3.69 (12H, d), 3.69–3.59 (36H, e), 3.58–3.52 (6H, f), 3.38–3.37 (9H, g), 1.31–1.28 ppm (9H, h); FT-IR (ATR): $\tilde{\nu}$ = 2872, 2246, 1769, 1717, 1597, 1505, 1539, 1437, 1370, 1299, 1239, 1181, 1111, 902, 847, 759, 704 cm^{-1}.

Amino terminated oligo(3-ureido-*N*-{3,4,5-tris[(2*S*)-2-(2-{2-[2-(2-methoxyethoxy)ethoxy]ethoxy}ethoxy)propoxy]phenyl}phthalimide-*N'*,6-diyl) (3): Under argon, a solution of 3,6-diaminophthalimide **1** (0.157 g, 0.152 mmol) and dry 4-dimethylaminopyridine (DMAP) (18.3 mg, 0.15 mmol) in dioxane (0.5 mL) was added to 3,6-diisocyanatophthalimide 2 (0.165 g, 0.150 mmol). The reaction mixture was heated to reflux overnight under continuous stirring followed by evaporation of the solvent in vacuo. The DMAP was removed by column chromatography (silica gel, 10 vol% MeOH in 1,2-dimethoxyethane) yielding a yellow-orange sticky solid (0.316 g, 95%). A second separation by column chromatography (silica gel, gradient from 1 to 10 vol% MeOH in 1,2-dimethoxyethane) afforded **3a** (0.153 g) containing the shorter oligomers, GPC ($CHCl_3$, mixed-E, 310 nm), t_R (min) = max. 5.69 min; and **3b** (0.140 g) containing the long oligomers as dark yellow sticky solids. **3b**; GPC ($CHCl_3$, mixed-E, 310 nm), t_R (min) = max. 4.73 and max. 4.35, tailing. ^{1}H NMR (400 MHz, $CDCl_3$, 25 °C): $\delta = 9.03$–8.70 ((4*n*+2)H, a and b),

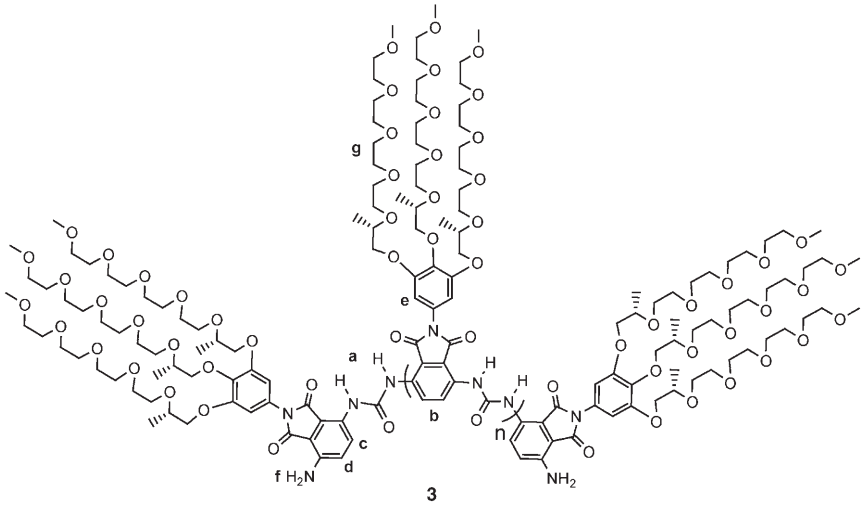

3

8.44 (d, 2H, ^3J(H,H) = 9.2 Hz, c), 6.98 (d, 2H, ^3J(H,H) = 9.2 Hz, d), 6.61–6.61 (2*n*H, e), 5.29 (s, 4H, f), 4.10–3.24, 1.32–1.28 ppm ((75*n* + 150)H, g).

Acknowledgements

The authors thank Xianwen Lou for MALDI-TOF MS analysis, Henk Eding for elemental analysis and Ralf Bovee for HPLC and GPC analyses and Stefan Meskers for useful discussion. NWO is acknowledged for the financial support.

[1] J. A. Kritzer, J. Tirado-Rives, S. A. Hart, J. D. Lear, W. L. Jorgensen, A. Schepartz, *J. Am. Chem. Soc.* **2005**, *127*, 167–178.
[2] Review articles on helical β-peptides: a) T. A. Martinek, F. Fülöp, *Eur. J. Biochem.* **2003**, *270*, 3657–3666; b) R. P. Cheng, S. H. Gellman, W. F. DeGrado, *Chem. Rev.* **2001**, *101*, 3219–3232; c) W. F. DeGrado, J. P. Schneider, Y. J. Hamuro, *Pept. Res.* **1999**, 54, 206–217.
[3] M. Reuping, Y. R. Mahajan, B. Jaun, D. Seebach, *Chem. Eur. J.* **2004**, *10*, 1607–1615.
[4] a) D. H. Appella, L. A. Christianson, I. L. Karle, D. R. Powell, S. H. Gellman, *J. Am. Chem. Soc.* **1996**, *118*, 13071–13072; b) D. H. Appella, L. A. Christianson, D. A. Klein, D. R. Powell, X. Huang, J. J. Barchi Jr., S. H. Gellman, *Nature* **1997**, *387*, 381–384.
[5] D. Seebach, J. L. Matthews, *Chem. Commun.* **1997**, 2015–2022.
[6] Review articles on foldamers: a) M. A. B. Block, C. Kaiser, A. Khan, S. Hecht, *Top. Curr. Chem.* **2005**, *245*, 89–150; b) A. R. Sanford, K. Yamato, X. Yang, Y. Han, B. Gong, *Eur. J. Biochem.* **2004**, *271*, 1416–1425; c) I. Huc, *Eur. J. Org. Chem.* **2004**, 17–29; d) C. Schmuck, *Angew. Chem.* **2003**, *115*, 2552–2556; *Angew. Chem. Int. Ed.* **2003**, *42*, 2448–2452; e) D. J. Hill, M. J. Mio, R. B. Prince, T. S. Hughes, J. S. Moore, *Chem. Rev.* **2001**, *101*, 3893–4011; f) S. H. Gellman, *Acc. Chem. Res.* **1998**, *31*, 173–180.
[7] J. Q. Nguyen, B. L. Iverson, *J. Am. Chem. Soc.* **1999**, *121*, 2639–2640.
[8] J. C. Nelson, J. G. Saven, J. S. Moore, P. G. Wolynes, *Science* **1997**, *277*, 1793–1796.
[9] X. Yang, L. Yuan, K. Yamato, A. L. Brown, W. Feng, M. Furukawa, C. X. Zeng, B. Gong, *J. Am. Chem. Soc.* **2004**, *126*, 3148–3162.
[10] a) B. Gong, *Chem. Eur. J.* **2001**, *7*, 4337–4342; b) J. T. Ernst, J. Becerril, H. S. Park, H. Yin, A. D. Hamilton, *Angew. Chem.* **2003**, *115*, 553–557; *Angew. Chem. Int. Ed.* **2003**, *42*, 535–539; c) H. Jiang, J. M. Léger, I. Huc, *J. Am. Chem. Soc.* **2003**, *125*, 3448–3449.
[11] Y. Hamuro, S. Geib, A. D. Hamilton, *J. Am. Chem. Soc.* **1996**, *118*, 7529–7541.
[12] a) V. Berl. I. Huc, R. G. Khoury, J. M. Lehn, *Chem. Eur. J.* **2001**, *7*, 2798–2809; b) C. Dolain, V. Maurizot, I. Huc, *Angew. Chem.* **2003**, *115*, 2844–2846; *Angew. Chem. Int. Ed.* **2003**, *42*, 2738–2740.
[13] P. S. Corbin, S. C. Zimmerman, P. A. Thiessen, N. A. Hawryluk, T. J. Murray, *J. Am. Chem. Soc.* **2001**, *123*, 10475–10488.
[14] J. L. Hou, X. B. Shao, G. J. Chen, Y. X. Zhou, X. K. Jiang, Z. T. Li, *J. Am. Chem. Soc.* **2004**, *126*, 12386–12394.
[15] H. Masu, M. Sakai, K. Kishikawa, M. Yamamoto, K. Yamaguchi, S. Kohmoto, *J. Org. Chem.* **2005**, *70*, 1423–1431.
[16] J. H. K. K. Hirschberg, L. Brunsveld, A. Ramzi, J. A. J. M. Vekemans, R. P. Sijbesma, E. W. Meijer, *Nature* **2000**, *407*, 167–170.
[17] L. Arnt, G. N. Tew, *J. Am. Chem. Soc.* **2002**, *124*, 7664–7665.
[18] L. Arnt, G. N. Tew, *Macromolecules* **2004**, *37*, 1283–1288.
[19] a) L. Brunsveld, E. W. Meijer, R. B. Prince, J. S. Moore, *J. Am. Chem. Soc.* **2001**, *123*, 7978–7984; b) R. B. Prince, L. Brunsveld, E. W. Meijer, J. S. Moore, *Angew. Chem.* **2000**, *112*, 234–236; *Angew. Chem. Int. Ed.* **2000**, *39*, 228–230.
[20] a) R. B. Prince, S. A. Barnes, J. S. Moore, *J. Am. Chem. Soc.* **2000**, *122*, 2758–2762; b) R. B. Prince, J. G. Saven, P. G. Wolynes, J. S. Moore, *J. Am. Chem. Soc.* **1999**, *121*, 3114–3121.
[21] M. T. Stone, J. S. Moore, *Org. Lett.* **2004**, *6*, 469–472.
[22] J. Garric, J. M. Léger, I. Huc, *Angew. Chem.* **2005**, *117*, 1990–1994; *Angew. Chem. Int. Ed.* **2005**, *44*, 1954–1958.
[23] A. Zhang, Y. Han, K. Yamato, X. C. Zeng, B. Gong, *Org. Lett.* **2006**, *8*, 803–806.
[24] J. J. van Gorp, J. A. J. M. Vekemans, E. W. Meijer, *Chem. Commun.* **2004**, 60–61.
[25] R. W. Sinkeldam, M H. C. J. van Houtem, G. Koeckelberghs, J. A. J. M. Vekemans, E. W. Meijer, *Org. Lett.* **2006**, *8*, 383–385.
[26] L. Brunsveld, H. Zhang, M. Glasbeek, J. A. J. M. Vekemans, E. W. Meijer, *J. Am. Chem. Soc.* **2000**, *122*, 6175–6182.
[27] H. M. Janssen, E. Peeters, M. F. v. Zundert, M. H. P. v. Genderen, E. W. Meijer, *Macromolecules*, **1997**, *30*, 8113–8128.
[28] a) K. Mori, *Tetrahedron* **1976**, *32*, 1101–1106; b) M. V. Perkins, W. Kitching, W. A. Köning, R. A. I. Drew, *J. Chem. Soc. Perkin Trans. 1* **1990**, 2501–2506; c) J. M. G. Cowie, H. W. Hunter, *Makromol. Chem.* **1990**, *191*, 1393–1401; d) E. Chiellini, G. Galli, S. Carrozzino, *Macromolecules* **1990**, *23*, 2106–2112.
[29] J. Shah, B. P. Conner, G. M. Swartz Jr., K. A. Hunsucker, J. Rougas, D. R. Amato, V. Pribluda, A. Teston, Patent WO 03014315, **2003**.
[30] K. R. Shoemaker, P. S. Kim, D. N. Brems, S. Marqusee, E. J. York, I. M. Chaiken, J. M. Steward, R. L. Baldwin, *Proc. Natl. Acad. Sci. USA* **1985**, *82*, 2349–2353.
[31] S. Marqusee, V. H. Robbins, R. L. Baldwin, *Proc. Natl. Acad. Sci. USA* **1989**, *86*, 5286–5290.
[32] R. B. Prince, L. Brunsveld, E. W. Meijer, J. S. Moore, *Angew. Chem.* **2000**, *112*, 234–236; *Angew. Chem. Int. Ed.* **2000**, *39*, 228–230.
[33] a) G. C. Barr, D. Norman, *Techniques Applied to Nucleic Acids: Nucleic Acids in Chemistry and Biology* (Eds.: G. M. Blackburn, M. J. Gait), 2nd ed., Oxford University Press, New York, **1996**, pp. 446–447; b) C. R. Cantor, P. R. Schimmel, *Biophysical Chemistry*, Freeman, New York, **1980**; c) V. A. Bloomfield, D. M. Crothers, I. Tinoco, *Physical Chemistry of Nucleic acids*, Harper & Row, New York, **1974**.
[34] a) S. Sakurai, K. Okoshi, J. Kumaki, E. Yashima, *J. Am. Chem. Soc.* **2006**, *128*, 5650–5651; b) K. Morino, K. Maeda, E. Yashima, *Macromolecules* **2003**, *36*, 1480–1486; c) H. Jiang, C. Dolain, J.-M. Leger, H. Gornitzka, I. Huc, *J. Am. Chem. Soc.* **2004**, *126*, 1034–1035.
[35] a) S. A. Wahab, H. Matsuura, *Phys. Chem. Chem. Phys.* **2001**, *3*, 4689–4695; b) R. Begum, T. Yonemitsu, H. Matsuura, *J. Mol. Struct.* **1998**, *447*, 111–117; c) R. Begum, H. Matsuura, *J. Chem. Soc. Faraday Trans.* **1997**, *93*, 3839–3848.
[36] A. L. Hofacker, J. R. Parquette, *Angew. Chem.* **2005**, *117*, 1077–1081; *Angew. Chem. Int. Ed.* **2005**, *44*, 1053–1057.

Received: April 4, 2006
Published online: June 23, 2006

